Whitmarsh, R.B., Sawyer, D.S., Klaus, A., and Masson, D.G. (Eds.), 1996
Proceedings of the Ocean Drilling Program, Scientific Results, Vol. 149

22. TECTONO-METAMORPHIC EVOLUTION OF PERIDOTITES FROM THE OCEAN/CONTINENT TRANSITION OF THE IBERIA ABYSSAL PLAIN MARGIN[1]

Marie-Odile Beslier,[2] Guy Cornen,[3] and Jacques Girardeau[3]

ABSTRACT

The drilling of peridotite during ODP Leg 149 confirms that the peridotite ridge, previously explored on the Galicia Margin, is a major feature continuous over more than 250 km in the ocean/continent transition of the west Iberian Margin. At Site 897, the ultramafic rocks are serpentinized spinel and plagioclase-bearing lherzolite and websterite, with minor harzburgite and dunite.

The serpentinized peridotites underwent four main events during their high-temperature evolution: (1) high temperature (1000°-900°C) shear deformation; (2) limited partial melting and (3) subsolidus reequilibration in the plagioclase stability field; and (4) poorly developed mylonitic shear deformation at a lower temperature (700°C), under high deviatoric stress and at low pressure (i.e., under lithospheric conditions). As for the Galicia peridotites, this evolution is compatible with mantle dome uplift beneath a continental rift zone, and it confirms that simple shear is a major deformation mechanism involved in extension of the continental lithosphere.

A complex deformation under subsurface conditions during the serpentinization of the rocks documents the late emplacement of the tectonically denuded dome at the rift axis. Hydrothermalism had an important role during this late evolution, which suggests that the mantle can be stretched over a large width after continental breakup, thus creating a wide (150 km) ocean/continent transition along the passive margin.

INTRODUCTION

The occurrence of serpentinized peridotite sampled at the ocean/continent transition of passive continental margins demonstrates that oceanic accretion does not immediately follow the continental breakup. Hence, mantle can rise up to the surface at the rift axis before the beginning of oceanic accretion and the subsequent formation of oceanic crust. At present, only a few examples of such occurrences are known. Mantle rocks have been sampled in or close to the ocean/continent transition in narrow basins such as the Red Sea (Zabargad Island—Bonatti et al., 1981, 1986; Styles and Gerdes, 1983; Nicolas et al., 1985, 1987) and the Tyrrhenian Sea (Bonatti et al, 1990; Kastens et al., 1986) and along the ocean/continent transition of large oceans: off southwest Australia (Nicholls et al., 1981) and off west Iberia (Boillot et al., 1980, 1988b; Girardeau et al., 1988; Beslier et al., 1990; Shipboard Scientific Party, 1993). Some ophiolite complexes, in particular in the western Alps in Queyras (France—Lemoine et al., 1987) and at Davos (Switzerland—Peters and Stettler, 1987), display comparable petrostructural characteristics, suggesting a former emplacement in such an extensional context. This concept of mantle emplacement near or at the surface associated with a rifting episode tends to be generalized. From seismic data, the presence of serpentinized mantle in the ocean/continent transition is also suggested on the conjugate margins of the Labrador Sea (Chian et al., 1994) and along the southern part of the west Iberian Margin in the Tagus Abyssal Plain (Pinheiro et al., 1992).

However, because of the scarcity of such known occurrences and the variety of regional contexts that prevailed during the rifting, the modalities of mantle uplift and of emplacement on the seafloor are poorly constrained, as are the mechanisms of thinning and breakup of the continental lithosphere during rifting. In the Red Sea, Nicolas et al. (1994) proposed a two-stage model of rifting. The first stage implies the intrusion of an asthenospheric wedge in the lithosphere that is submitted to a transcurrent regional regime and then a final emplacement of the peridotite on the seafloor during a second stage of oblique rifting and thinning of the crust. On the Galicia Margin, Boillot et al. (1988b) and Beslier and Brun (1991) proposed progressive uplift of a mantle dome during stretching of the lithosphere and a final tectonic denudation of the dome along lithospheric ductile shear zones during its ascent through the crust.

During Ocean Drilling Program (ODP) Leg 149, peridotite was recovered in three holes (Holes 897C, 897D, and 899B) at the top of a structural ridge in the ocean/continent transition of the Iberia Abyssal Plain, which is the southward prolongation of the Galicia Margin. This shows that the peridotite ridge is a major feature of the west Iberia passive margin, which forms a continuous belt in the ocean/continent transition over a north-south distance of at least 300 km. This paper presents a structural study of the peridotites of the Iberia Abyssal Plain in order to define their deformation history. This evolution, in relation to the structural setting of the ridge and the structure of the ocean/continent transition in this segment of the margin, will help to constrain the mechanisms of mantle uplift and emplacement at a rift axis during the first stage of formation of an ocean.

REGIONAL BACKGROUND

The peridotite ridge of the west Iberian Margin was first discovered on the Galicia Margin (Fig. 1). Sampling by dredging (Boillot et al., 1980), drilling (ODP Leg 103; Boillot, Winterer, Meyer, et al., 1988), and diving with the French submersible *Nautile* (Galinaute cruise; Boillot et al., 1988a) have demonstrated that mantle rocks form a continuous belt at the ocean/continent transition. Petrostructural studies of these plagioclase-bearing peridotites show that their evolution is compatible with uplift under a rift zone. They were submitted to an early high-temperature metamorphic event expressed by

[1]Whitmarsh, R.B., Sawyer, D.S., Klaus, A., and Masson, D.G. (Eds.), 1996. *Proc. ODP, Sci. Results,* 149: College Station, TX (Ocean Drilling Program).

[2]Laboratoire de Géodynamique Sous-Marine, URA 718 CNRS-Université Paris 6, B.P. 48, F-06230 Villefranche-sur-Mer, France, beslier@ccrv.obs-vlfr.fr

[3]Laboratoire de Pétrologic Structurale, Université de Nantes, 2 rue de la Houssinière, F-44072 Nantes cedex 03, France.

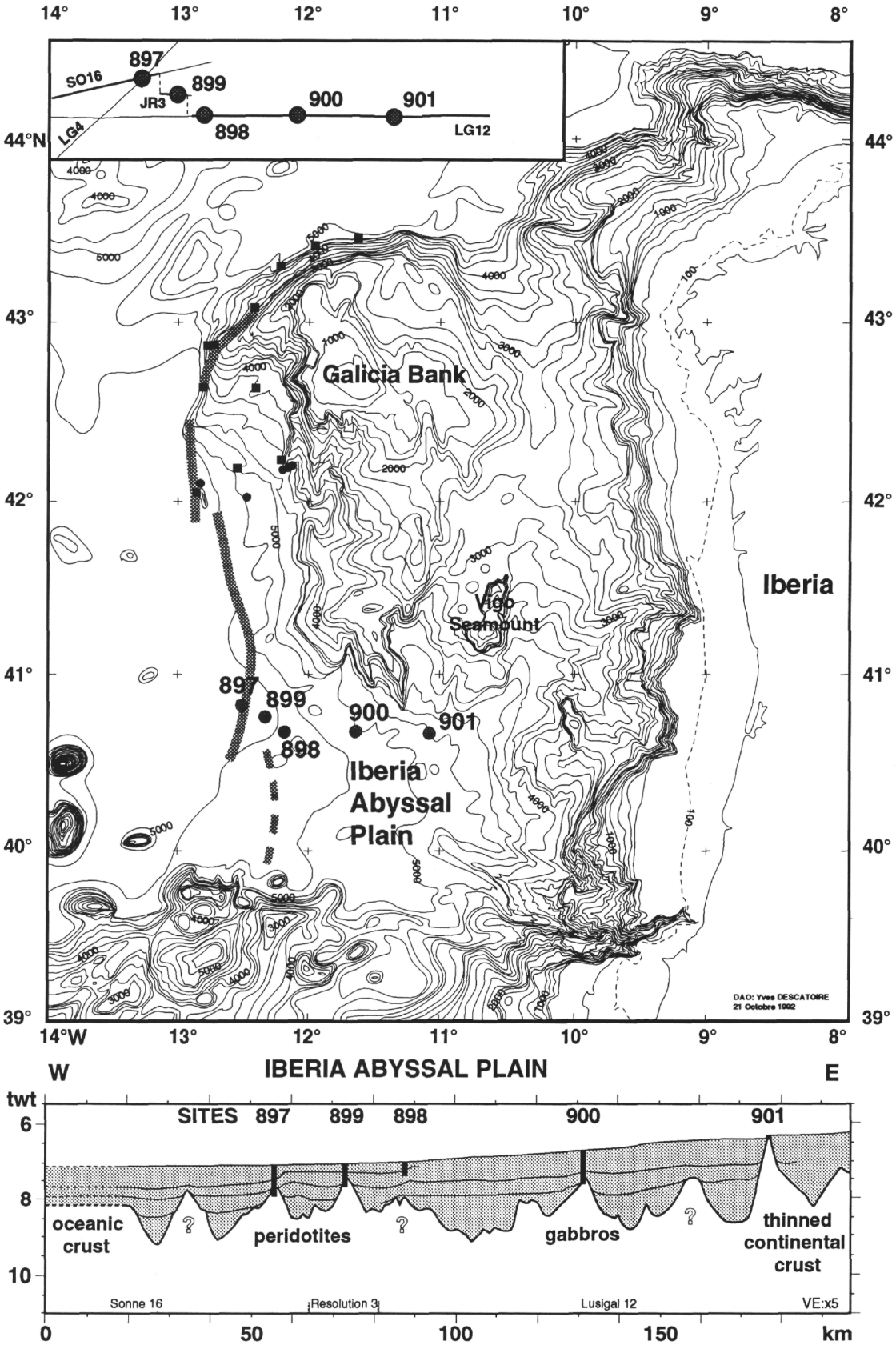

Figure 1. Bathymetric map of the west Iberia Margin (Lallemand et al., 1985) and schematic cross section of the Iberia Abyssal Plain. The peridotite ridge (gray line) and Sites 897-901 of Leg 149 are shown. On the Galicia Margin, solid circles are for ODP Leg 103 sites and solid squares are for diving sites of the Galinaute cruise. The inset map at the top shows the location of the seismic lines (LG and SO: *Lusigal* 90 and *Sonne* 75 cruises; JR: Leg 149) used to construct the synthetic cross section.

low partial melting (7%) and plastic deformation (Evans and Girardeau, 1988; Girardeau et al., 1988). Most of the rocks, locally intruded by dioritic dikes, display mylonitic to ultramylonitic textures acquired during shearing at high and decreasing temperatures (1000° to 850°C) in the plagioclase stability field (<1 GPa) and under high deviatoric stresses (>100 MPa) (i.e., under lithospheric conditions) (Beslier et al., 1990; Girardeau et al., 1988). Dating of the Syntectonic recrystallization in the intrusive dikes gives an age of 120 Ma for the end of the mylonitization (Boillot et al., 1989; Féraud et al., 1988). As the breakup unconformity on the adjacent margin is of late Aptian age (Mauffret and Montadert, 1987; Sibuet et al., 1987), the emplacement of peridotite in the lithosphere is coeval with the rifting-phase episode. In the southern part of the margin, the shear deformation occurred along a normal shear zone dipping toward the continent. The late evolution of these rocks is characterized by serpentinization and a brittle deformation that is coaxial with the earlier ductile one (Agrinier et al., 1988; Girardeau et al., 1988).

These data, the geological setting of the ridge, and the structure and evolution of the margin, as well as the results of small-scale analogical models, have been integrated into a model of formation of the margin (Beslier, 1991; Beslier and Brun, 1991). Stretching of the lithosphere involves boudinage of the brittle layers (upper crust and uppermost mantle) and the coeval development of two conjugate normal shear zones in the weaker ductile layers, one in the lower crust and one in the lithospheric mantle. A mantle dome rises simultaneously beneath the stretched zone. While rifting is in progress, extension tends to localize in the rift axis, where extreme thinning of the lithosphere leads to tectonic denudation of the mantle dome.

In the Iberia Abyssal Plain, as a consequence of the northward propagation of the opening of the North Atlantic Ocean (Mougenot, 1989; Pinheiro et al., 1992), lithospheric breakup occurred earlier than on the northern Galicia Margin (beginning of Chron M3, 125 Ma according to the time scale of Kent and Gradstein, 1986; Whitmarsh et al., 1990). Whitmarsh et al. (1990, 1993), from refraction data, and Beslier et al. (1993), from reflection seismic data, predicted that the Galicia peridotite ridge is prolonged southward in the Iberia Abyssal Plain. However, it shifts toward the east in this part of the margin (Fig. 1). This segmentation of the ridge may reflect a discontinuous propagation of the continental breakup toward the north between the Iberian and North American plates. On the landward side of the peridotite outcrops, in a 120-km-wide area where the upper part of the basement was previously interpreted as thin continental crust (Whitmarsh et al., 1990), peridotitic breccia and sheared gabbros were drilled at Holes 899B and 900A, respectively, during Leg 149 (Fig. 1; Shipboard Scientific Party, 1993; Sawyer, Whitmarsh, Klaus, et al., 1994). On the seismic reflection lines, the basement in this area is structured in north-south-trending ridges, which do not display the typical asymmetrical shape of tilted blocks (Beslier et al., 1993; 1995). Compared to the Galicia Margin, where the first continental tilted block is located 20 km east of the peridotite ridge (Boillot et al., 1988a, 1988b), the structural setting of the mantle outcrops and structure of the ocean/continent transition are not similar on the two adjacent segments of the west Iberian Margin.

PERIDOTITES OF HOLES 897C AND 897D

Lithologic Data

Two holes, 897C and 897D, separated by 100 m, were drilled through a 650- to 690-m-thick sedimentary cover of Pleistocene to Hauterivian age, down to the basement, which is composed of serpentinized peridotite. In Hole 897C, 96.2 m of basement was drilled with 33.8% recovery, and 152.9 m was drilled in Hole 897D with 54% recovery.

Three sedimentary intervals in Hole 897C and one in Hole 897D separate intervals of altered peridotite in the lowest sedimentary unit overlying the basement (Unit IV). This unit is tentatively interpreted as a mass-flow deposit at the top of the basement (Sawyer, Whitmarsh, Klaus, et al., 1994).

The entire ultramafic section in both holes is extensively serpentinized. The rocks are generally pale green or black, except the plagioclase-rich peridotite, which is gray. In addition, the upper part of the basement in Hole 897D is pervasively calcitized and altered (up to 99%) and is yellow to brown in color (Sections 149-897D-10R-3 to 15R-2 and 16R-4 to 16R-7). This late calcitization overprints most of the previous structures in the rocks. As the lower limit of the calcitized zone at 742 m below seafloor (mbsf) corresponds to the base of Hole 897C (744.9 mbsf), no correlation of primary features between the two holes is possible.

Tectonic brecciation is extensive and unevenly distributed throughout the cores from both holes. Although several types of breccia were distinguished, all result from a local intense fracturing of the basement.

The recovered peridotites display various lithologies, which point out the initial heterogeneity of the mantle. A detailed description is given in Sawyer, Whitmarsh, Klaus, et al. (1994), Cornen et al. (chapter 21, this volume) and Agrinier et al. (this volume). The main types recovered are spinel-bearing dunites and harzburgites and spinel- and plagioclase-bearing harzburgites, lherzolites, and websterites.

Aboard ship, almost no high-temperature ductile deformation was observed in the peridotite, as the primary texture of the rocks appears to be equant. However, evidence for such a "primary" deformation is shown by the shore-based microstructural study. The breccias and the extensive fracturing observed in the cores are evidence of a late low-temperature deformation of the serpentinized peridotite.

Structural and Microstructural Data

High-temperature Primary Deformation

One hundred samples from Site 897 (Holes 897C and 897D) were studied in addition to the shipboard thin sections, which were reexamined in detail. Approximately 200 new thin sections were cut in order to determine the main deformation planes (xy, yz, and xz) and then to study the rocks in these planes.

Two main facies were sampled in the cores, namely serpentinized peridotite, with various proportions of pyroxenes and plagioclase, and plagioclase-rich websterite, as banding of the previous facies. Calcitization, in the shallowest cores, and serpentinization and late ductile shear and brittle deformation, at all depths, commonly overprint the primary texture of these rocks. However, although the peridotite is generally totally serpentinized, the websterite is generally well preserved (serpentinization averaging 30%).

Primary Textures

The dominant texture of the peridotites and the websterites at Site 897 is porphyroclastic, although it is locally mylonitic and ultramylonitic.

In thin section, the websterites generally have a large grain size (10 mm) and display a spinel-plagioclase foliation and lineation and small amounts of recrystallization. In the freshest facies, olivine and orthopyroxene porphyroclasts display kink bands (Pl. 1; Figs. 1, 2). Some rare orthopyroxene crystals are poorly stretched by gliding along the slip system (100) [001] visualized by thin exsolution lamellae (Samples 149-897C-64R-5, 95 cm, and 67R-3, 120-125 cm; Pl. 1, Fig. 1). The kinking of such elongated crystals may provide evidence of some rotation of the stress field during the deformation. The exsolution lamellae seen in both pyroxene crystals are usually distorted in clinopyroxene (Pl. 1, Figs. 3, 4). Some recrystallization of olivine and pyroxenes occurs preferentially at grain boundaries (Sample 149-897C-64R-5, 95 cm; Pl. 1, Fig. 4) and along kinks (Sample 149-897C-67R-1, 95 cm). These features are evidence of high-temperature ductile shear deformation, in good agreement with the intracrystalline fabric of olivine crystals (see "Physical Conditions of Deformation" section; Carter, 1976; Nicolas and Poirier, 1976; Mercier, 1985).

Generally, however, orthopyroxene and clinopyroxene crystals are poikilitic and display resorption features (Pl. 1, Figs. 1, 3). Secondary orthopyroxene blebs also occur in clinopyroxene exsolution lamellae in association with plagioclase (Pl. 1, Fig. 4), and plagioclase crystals are interfingered with secondary olivine between former pyroxene porphyroclasts. These observations suggest a subsolidus reequilibration of the websterite under plagioclase facies conditions (Cornen et al., chapter 21, this volume). Deeply lobate pyroxene porphyroclasts displaying kink bands show that pyroxene resorption postdates the formation of the kink bands. However, in the clinopyroxene exsolution lamellae, the plagioclase crystals display mechanical twins, and secondary orthopyroxene crystals display undulose extinction or even kink bands (Pl. 1, Fig. 4; Samples 149-897C-64R-5, 95 cm, 67R-3, 31 cm, and 67R-3, 97 cm). This suggests that reequilibration occurred at the end of and after the high-temperature deformation event.

The proportion of plagioclase is generally high and varies from 5% to 35%. Plagioclase occurs mainly in thin veinletlike ribbons (1-2 mm thick). In plagioclase-rich facies, these veinlets are not recognizable, and plagioclase forms interstitial patches (Pl. 1, Fig. 2). This suggests the local presence of plagioclase melt in the rocks. In the ribbons, plagioclase is partially recrystallized. It forms large crystals (2 mm) displaying bulge features locally (Sample 149-897C-64R-5, 95 cm) or small neoblasts (0.1 mm) with triple junctions in the most recrystallized facies (Samples 149-897C-66R-4, 60 cm, and 66R-4, 68 cm). Mechanical twins are visible in both porphyroclasts and neoblasts. Where present, the interstitial plagioclase veinlets are elongate and aligned along two directions, with one more developed than the other. This pattern, outlined by elongate spinel crystals, defines foliation and lineation in the rocks (Pl. 1, Figs. 1, 2). Locally, however, the complexity of the veinlet pattern prevents a precise determination of their attitude (see below).

In the peridotite surrounding the websterite, some evidence of a high-temperature deformation event is still recognizable in the pyroxene ghosts of serpentinized facies (kink bands, distorted exsolution lamellae), and some rare fresh samples display a porphyroclastic texture similar to that of the websterite (Samples 149-897D-19R-5, 83 cm, and 23R-6, 85 cm). Pyroxene crystals display resorption features, even if kinked, and small neoblasts are developed locally at grain boundaries. The preservation of large kinked olivine crystals (6 mm) suggests that deformation was not much more intense in the peridotitic facies than in the pyroxenitic ones.

In both peridotites and websterite, the foliation marked by elongate spinel crystals and plagioclase veinlets is mostly concordant or slightly oblique to the ductile high-temperature fabric marked by kink-band boundaries and a few elongated orthopyroxene crystals (Pl. 1, Figs. 1, 2; e.g., Sample 149-897C-67R-3, 122 cm). Where two spinel-plagioclase alignment planes are identified, one is the foliation plane, and the other corresponds to the shear plane, associated with the slip plane of the olivine crystals determined from petrofabric analysis. Moreover, the spinel-plagioclase lineation is close to the shear direction. This concordance between the ductile fabric and the spinel-plagioclase fabric shows that the crystallization of plagioclase melts is controlled by high-temperature deformation.

Mylonitic and ultramylonitic textures were also observed locally in shear zones within the cores (e.g., Sample 149-897C-67R-3, 52-65 cm). Deformation in such zones is highly heterogeneous, with cores of porphyroclastic websterite preserved between anastomosing mylonitized bands (Pl. 1, Fig. 5; e.g., Sample 149-897C-67R-3, 45 cm). These bands are characterized by the recrystallization of olivine and plagioclase neoblasts (0.2 mm) in elongate ribbons and of pyroxenes to a lesser extent. Some orthopyroxene crystals are elongated along their exsolution planes. Spinel is surrounded by plagioclase and displays lobate boundaries, which suggests resorption of the crystals. These resorbed crystals, embedded in plagioclase neoblast ribbons, are commonly granulated and elongate (Pl. 1, Fig. 6).

Mylonitic foliation and lineation are marked by the elongate spinels and the neoblast ribbons. These structures appear to be concordant with the high-temperature foliation and lineation in the adjacent porphyroclastic facies (Pl. 1, Fig. 5; Sample 149-897C-67R-3, 45 cm).

These mylonitic bands are crosscut at a few degrees (20°) by narrow (1 mm thick) ultramylonitic bands in which the size of the olivine, plagioclase, and pyroxene neoblasts is significantly reduced (<0.01 mm; Pl. 1, Figs. 5, 6) and spinel is completely granulated and separate (Sample 149-897C-67R-3, 45 cm). As in the Galicia Margin peridotites, these bands are interpreted as shear bands (Girardeau et al., 1988). In a few places, only a network of ultramylonitic narrow bands crosscuts the porphyroclastic rocks. These shear zones have sharp limits, suggesting that the deformation evolved toward a lower temperature cataclastic regime.

Green to colorless amphiboles occur in the mylonitic zones, either replacing pyroxene crystals or in straight veinlets parallel or oblique to the foliation. This postkinematic crystallization of amphiboles, not observed in the porphyroclastic facies, suggests that mylonitic zones are zones of later preferential circulation of fluids.

Mylonitic bands have been observed only in the plagioclase-rich facies, mainly in websterite layers, and rarely in the surrounding peridotites. As plagioclase is easier to deform than the surrounding pyroxene and spinel in these conditions, this suggests that the mylonitization occurred after the plagioclase crystallization and tended to localize in the weaker plagioclase-rich zones. Spinel resorption, clearly observed in the mylonitic and ultramylonitic bands, suggests that the mylonitic deformation occurred in the plagioclase stability field (i.e., at a rather shallow depth, probably near the Moho).

Physical Conditions of Deformation

To enable discussion of the deformation conditions, we conducted a petrofabric analysis of the olivine.

A representative petrofabric of the olivine porphyroclasts in a websterite is shown in Figure 2A. The relatively scattered data may be due to the rather low proportion of olivine crystals in the websteritic facies, which does not favor a homogeneous deformation of olivine. The [010] crystallographic axis is oriented at a high angle to the foliation and the [100] axis is close (30°) to the spinel-plagioclase lineation. This angle may be due to an imprecision in the determination of the lineation trend. Such a fabric indicates that the deformation occurred in a rotational regime by translation glide according to the (010)[100] slip system, which is activated at high temperature (>1000°C for geological strain rates; Carter and Avé Lallemant, 1970; Mercier, 1985). The shear sense inferred from these petrofabric diagrams, using the obliquity between the foliation plane and the (010) slip plane (Nicolas and Poirier, 1976), indicates a dextral movement. When replaced in the core reference frame, it shows that deformation occurred in a strike-slip shear zone with a normal component of displacement (lineation pitch = 28°; Fig. 3).

Figure 2B shows the olivine petrofabric in a mylonitic websterite. The crystallographic orientation was measured for three populations of olivine crystals: the porphyroclasts (Fig. 2B, 1), the neoblasts of the mylonitic shear zones (Fig. 2B, 2), and the very fine-grained neoblasts of the ultramylonitic shear bands (Fig. 2B, 3). Because of the relatively low proportion of olivine in such facies, the diagrams are based on only 20 to 32 data points. However, we believe that they are indicative of the strain regime, with each point plotted corresponding to a distinct crystal, whereas adjacent subgrains, formed by subgrain rotation (SGR; Nicolas and Poirier, 1976), are systematically ignored. We believe that such diagrams are much more representative than diagrams with 50 or more points, where most of them represent subcrystals derived from a few larger ones by SGR (Nicolas and Poirier, 1976). The petrofabric of the porphyroclasts is comparable to the one previously described, with the high-temperature (010)[100] slip system activated in a rotational regime. This is in agreement with the

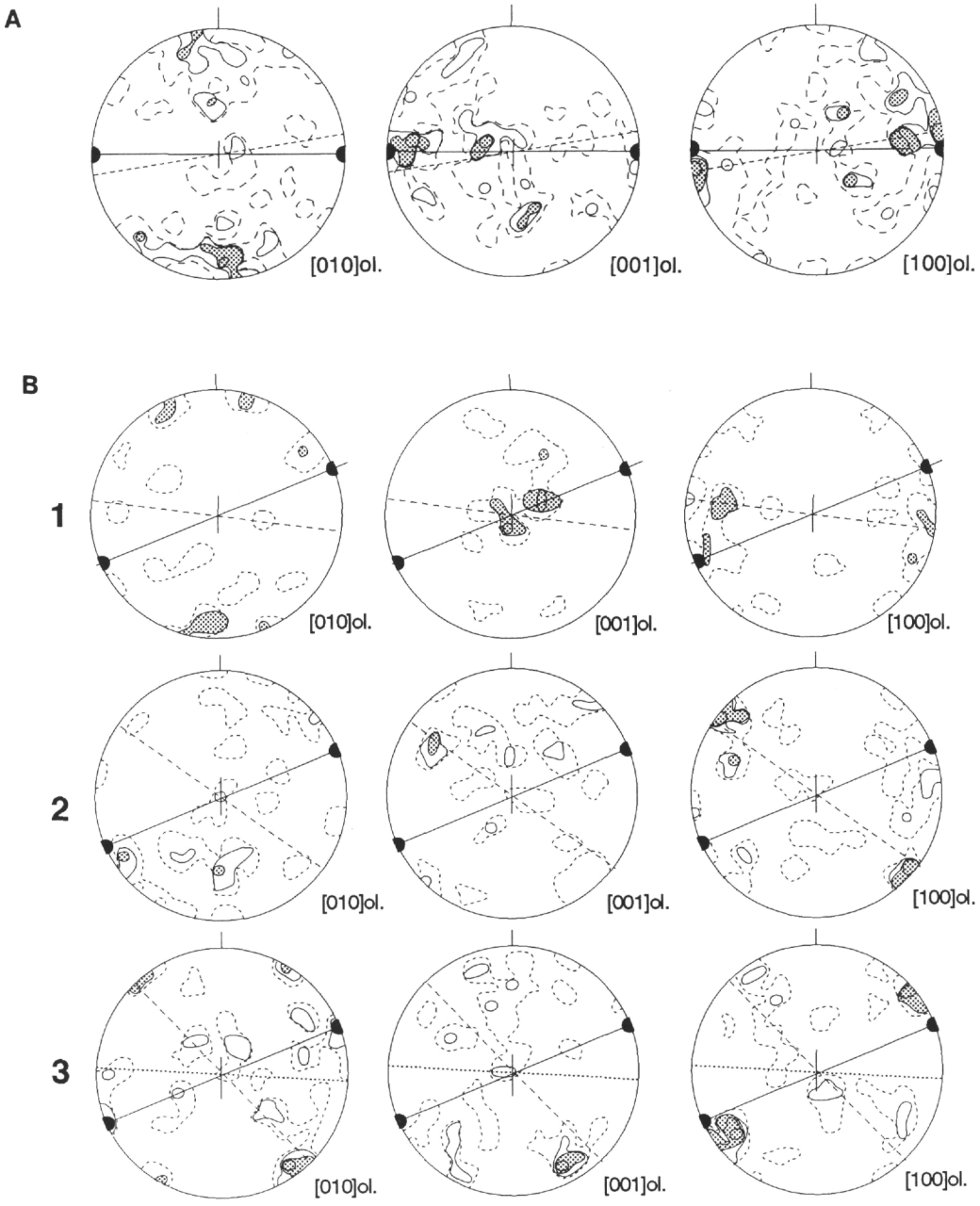

Figure 2. Olivine petrofabric diagrams (equal-area projection, lower hemisphere, line = trace of foliation, solid dots = lineation, dotted line = trace of shear bands, dashed line = inferred gliding plane). These diagrams plot the orientation of the [010], [001], and [100] crystallographic axes. **A.** Sample 149-897C-67R-2, 140 cm; n = 50; contours for 16%, 12%, 8%, and 4%. **B.** Sample 149-897C-67R-3, 45 cm; 1: porphyroclasts, n = 20, contours for 75%, 50%, and 25%; 2: neoblasts in mylonitic shear zone, n = 30, contours for 33%, 20%, and 10%; 3: neoblasts in ultramylonitic shear band, n = 32, contours for 50%, 40%, 31%, 18%, and 9%.

high-temperature (100)[001] slip system activated in the rare orthopyroxene porphyroclasts. The neoblasts in the shear zones show a more scattered petrofabric, which makes an unambiguous interpretation difficult because of the small amount of data (30). Maxima for the [100] and [010] axes are compatible with the activation of the high-temperature (010)[100] slip system. However, secondary maxima for the [100] and [001] axes suggest that the (100)[001] slip system may also have been active during the mylonitic deformation. This latter system is characteristic of lower temperature conditions (<600°-800°C; Carter and Avé Lallemant, 1970; Mercier, 1985). Conversely, in the ultramylonitic shear bands, better maxima are defined for the [100] and [001] axes compatible with a low-temperature (100)[001] slip system, and the dispersion of the data may be due to preserved traces of a high-temperature petrofabric or to too small a number of data points.

The systematic obliquity between slip and foliation planes on the petrofabric diagrams also suggests that the deformation is rotational. The inferred dextral shear sense is the same for the porphyroclastic and the mylonitic deformation events (Fig. 2B). Shear sense is confirmed by the obliquity of the ultramylonitic bands, which are interpreted as shear bands (Pl. 1, Fig. 5). Hence, the mylonitic deformation is coaxial with the high temperature deformation event. When re-

placed in the core reference frame, such a shear sense indicates that the websterite has been deformed in a strike-slip shear zone with a reverse component (lineation pitch = 40°; Fig. 3).

From textural relationships, mylonitic features clearly overprint the porphyroclastic texture. Petrofabric analysis strongly suggests that mylonitization occurred at a lower temperature (600°-800°C) than the previous porphyroclastic deformation event (≥1000°C; Carter and Avé Lallemant, 1970). These data, implying decreasing temperatures, are in good agreement with equilibrium temperatures calculated by Cornen et al. (chapter 21, this volume). Accordingly, a temperature of 965° to 880°C could reflect the physical conditions at the end of the high-temperature deformation responsible for the porphyroclastic texture, and a temperature of 735°C for the end of the mylonitic deformation event. Moreover, the grain-size reduction of the neoblasts indicates an increasing deviatoric stress during the deformation evolution (Mercier, 1985). A coeval pressure decrease during evolution of the mantle rocks is inferred from the last reequilibration in the plagioclase facies conditions (i.e., at pressures below 1 GPa).

Orientation of Structures

Formation MicroScanner data were not acquired in the basement of either Hole 897C or Hole 897D, and paleomagnetic data are available only for Hole 897D, where almost no fresh facies were recovered. Hence, it is not possible to reorient cores or to orient the structural features in the geographical frame. Consequently, the foliation dip and lineation pitch may be the only significant data relative to the kinematics of the deformation. The orientation of the main deformation planes, when well expressed, has been determined after several cuts in a few selected samples.

The data, which are reported in Figure 3, show that the attitude of the structures is highly variable. The foliation dip and the lineation pitch may be not significant for the six uppermost samples of Hole 897C (Samples 149-897C-64R-5, 53 cm, to 65R-1, 110 cm; Fig. 3), which belong to the unit tentatively interpreted as a mass-flow deposit at the top of the basement. For the other samples, the foliation dip varies from 30° to 80° with a mean of 51°, which is rather steep. The variability of the lineation pitch is even larger. The pitch varies from 0° to 90° with a mean of 54°. These measurements document a local strike-slip component. A striking result is the shear sense, determined for only a few of the freshest samples on petrofabric diagrams. In addition, even though it is not consistent for all samples, three determinations indicate a reverse shear sense (Samples 149-897C-64R-5, 53 cm, 64R-5, 105 cm, and 67R-3, 46 cm) and one, which is less reliable because of the small size of the sample, a normal shear sense (Sample 149-897C-67R-2, 141 cm), all with a strike-slip component.

However, a ubiquitous late deformation can be observed at every depth in the recovered cores. It is expressed as fracturing and ductile shearing of the rocks (see "Secondary Late Deformation" section). Where intense, this late deformation was responsible for brecciation of the rocks, and some shear zones may have accommodated large displacements in the mantle. This possibly could have disturbed and rotated the primary structures previously acquired at a greater depth and tentatively explains, at least partly, the dispersion of orientations of the primary structures.

Secondary Late Deformation

The primary texture was overprinted in many places by an extensive low-temperature deformation during the serpentinization of the peridotites. This deformation is usually difficult to observe as it tends to weaken the rocks, which are consequently hardly recoverable by drilling. Features associated with this deformation include (1) fractures and brecciation of the serpentinized peridotite and (2) shear zones in serpentinite. We present here a synthesis of the main features previously detailed in the "Structural Geology" section of the "Site 897" chapter in Sawyer, Whitmarsh, Klaus, et al. (1994) and new shore-based data.

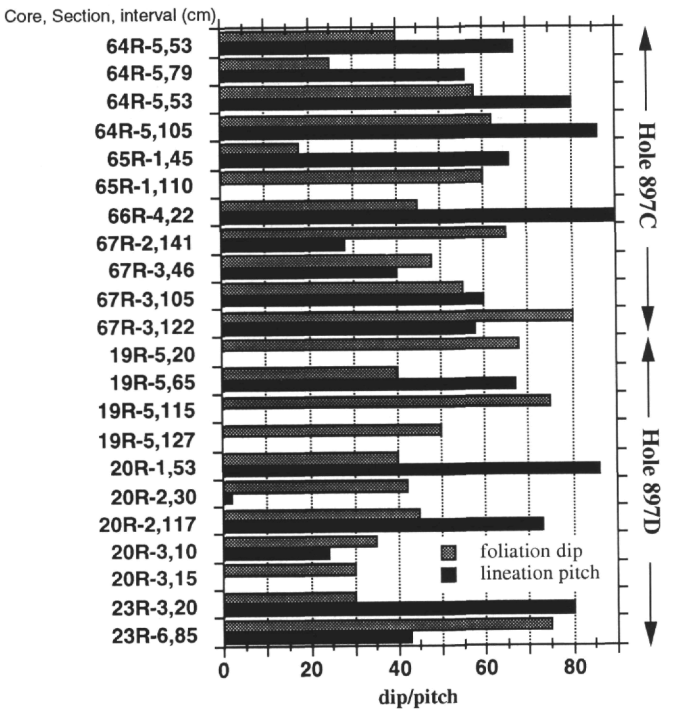

Figure 3. High-temperature foliation dip and lineation pitch (degrees) measured in selected samples of Holes 897C and 897D. No values are where no measurement was possible because of extensive serpentinization.

Fracturing

Although extensive and expressed at every depth, fracturing is unevenly distributed throughout the cores. The fractures are filled mainly with calcite and serpentine, although minor opaque and brucite fillings also exist. In both Holes 897C and 897D, the dominant filling mineral progressively changes downward from calcite to serpentine. Although the serpentine filling displays various colors and habits, it formed mainly at low temperature, according to Agrinier et al. (this volume).

Three main types of fracture are distinguished on the basis of their geometry:

1. Generally planar 0.1- to 15-cm-thick fractures, continuous over the width of the core, that are filled with calcite and/or serpentine. The general vein pattern suggests that the fractures show two sets of conjugate directions, with one set preferentially developed (Samples 149-897C-63R-2, 40-145 cm, and 67R-2, 7-30 cm, and Section 149-897D-16R-5). Dips vary from 30° to 75° with two maxima at about 45° and 60°. Some subhorizontal and subvertical fractures were also observed. Where the fracture density is high, the rocks are brecciated and display angular serpentinized peridotite blocks embedded in a calcite and/or serpentine matrix (Fig. 4; Samples 149-897C-64R-4, 55-65 cm, and 65R-1, 3-97 cm). They are similar to ophicalcite-type breccias described in the western Alps ophiolite massifs as occurring as thick layers at the top of the basement, under the oldest sedimentary layers (Lemoine et al., 1987). Deeper in the basement locally, the blocks are embedded in a folded and convoluted serpentine matrix (Sample 149-897D-19R-3, 73-105 cm). This fracturing is extensively developed in the upper parts of both Holes 897C and 897D, where the freshest, or calcitized, facies is recovered, and is absent in deeper levels (below 710 and 780 mbsf, respectively), where peridotite is highly serpentinized. The overall vein pattern is compatible with a brittle behavior of the rocks in a hor-

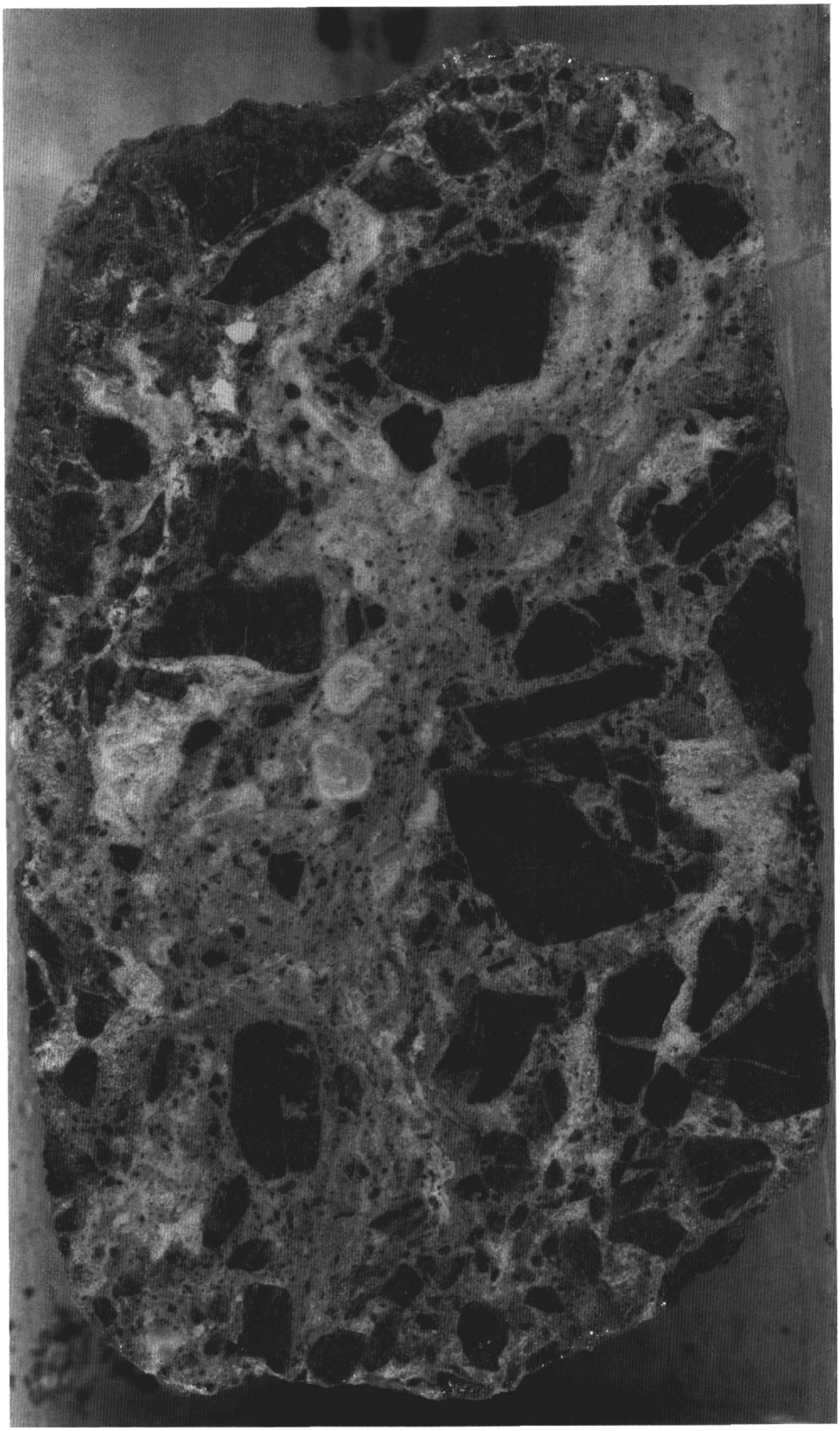

Figure 4. Ophicalcite-type breccia in Sample 149-897C-64R-4, 55-65 cm: clasts of serpentinized peridotite in a calcite/serpentine matrix.

izontal extensional regime. Textural relationships show that calcite-filled fracturing is the latest main fracturing event. Locally, however, some rare thin fractures filled with cataclastic microbreccia crosscut the calcite veins.

2. Sinuous veins filled either with white massive serpentine or with pale green fibrous serpentine. Both types are coeval and distributed unevenly in the deeper half of both holes. Locally, they were initiated on heterogeneities in the rocks as bastitized pyroxene crystals or clusters (e.g., Samples 149-897D-20R-1, 20-95 cm, and 21R-2, 20-38 cm). With increasing vein density, they are aligned along a preferential dipping plane (45°-60°; e.g., Sections 149-897C-73R-4 and 897D-23R-5). They usually display sigmoidal shapes characteristic of tension gashes that have a geometry is in accordance with horizontal extension (Figs. 5, 6; e.g., Samples 149-897C-70R-2, 50-90 cm, 897D-22R-2, 75-110 cm, and 897D-23R-6, 70-95 cm). Locally, the deformation appears to grade into penetrative deformation, leading to fracture cleavage (Sample 149-897C-71R-2, 22-33 cm) or to an anastomosing pattern that outlines rhomboidal clasts of serpentinized peridotite (e.g., Samples 149-897C-71R-2, 116-127 cm, and 897D-21R-4, 9-31 cm). This anastomosing pattern appears to result from initially sigmoidal veins that were rotated and aligned along planes dipping from 60° to 40° (Fig. 6; Sample 149-897C-70R-2, 50-90 cm). This attests to a rotational extensional regime. Such intervals rich in serpentine are precursors of shear zones.
3. Thin (1 mm) irregular veins filled either with calcite in the upper calcitized part of Hole 897D (Section 149-897D-12R-5) or with serpentine below Section 12R-5 and in Hole 897C (Fig. 7A; Section 149-897C-73R-3 and Sample 149-897D-18R-1; 65-150 cm). These veins display an unusual contorted habit and permeate the rock, suggesting that hydrothermal fluid circulation may have aided fracturing. This is supported by the presence of typical hydrothermal minerals in these zones, either as thin fractures filled with brucite associated with the calcite veins or as iowaite associated with serpentine. Although these veins are generally aligned along planes dipping from 30° to 65° (Fig. 7A; e.g., Samples 149-897D-12R-4, 45-75 cm, and 897C-73R-3, 10-60 cm), they are locally subhorizontal (Fig. 7A; e.g., Sample 149-897C-73R-3, 110-145 cm) or display no preferential orientation (e.g., Samples 149-897D-12R-5, 70-115 cm, and 18R-1, 75-95 cm). Such variation of fracture orientation, suggesting a local change of the stress field, is possibly due to local fluid overpressure.

Where vein density is high, small isolated rounded elements define a brecciated texture in the rocks (Fig. 7A; e.g., Samples 149-897D-12R-3, 90-120 cm, and 897C-73R-3, 105-135 cm). Thick (at least 1 to 3 m, considering the poor recovery in soft materials) breccia intervals recovered in both holes display this texture, as described below:

1. In Sections 149-897D-17R-4 through 6 and the top of Section 18R-1 (Fig. 7B), it can be locally identified, although later fracturing extensively overprints previous features. Locally, where the serpentine proportion is dominant, the rounded elements are rotated in the sheared serpentine matrix (Samples 149-897D-18R-1, 103-110 cm, and 17R-4, 40-55 cm). Late fracturing, which is coaxial with the shearing, is expressed as a set of tight parallel calcite and locally as brucite veins dipping at 45°. Remobilization of serpentinite breccias by calcite fracturing clearly demonstrates that the rocks underwent a multistage complex low-temperature evolution.
2. Friable serpentinite breccias recovered in Section 149-897D-10R-2 and in subjacent Sample 140-897D-10R-3, 0-40 cm, are also made of rounded serpentinite clasts individualized by contorted veins filled with a pale serpentine-like mineral (Fig. 7C). The friability of this material may be due to further pervasive alteration. Although sheared, the overall texture of two other thick friable serpentinite breccia intervals is comparable (Sections 149-897C-66R-1 to 3 and 897D-18R-2 to 4). Here, the smaller mean size of the clasts may be due to further shear deformation. A similar origin is thus proposed for all these soft breccias. However, they display also some similarities with serpentine sediments described from serpentine mud volcanoes in the Izu-Bonin-Mariana forearc (Fryer, Pearce, Stokking, et al., 1990).

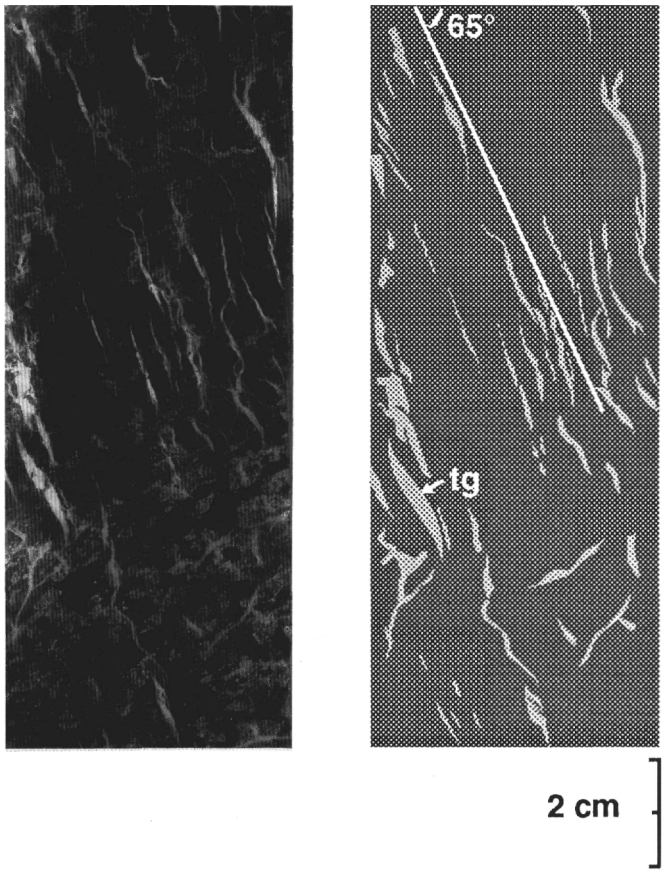

Figure 5. Sigmoidal tension gashes (tg) filled with white massive serpentine and aligned along a plane dipping at 65°; Sample 149-897D-23R-6, 75-89 cm.

Shear Deformation

Low-temperature shear zones occur mainly in the deeper half of both holes. Unevenly distributed, they are localized in intervals of high serpentine vein density and formed subsequent to intense fracturing. The veins mark a plane of schistosity dipping at about 30°, which is oblique to coeval shear bands (S/C fabric; Fig. 8; e.g., Sample 149-897C-71R-2, 116-127 cm). Shear zones 5 to 50 cm thick also occur in blue serpentinites (Fig. 9; e.g., Samples 149-897D-19R-1, 1-50 cm, 19R-1, 80-120 cm, 21R-2, 108-114 cm, and 21R-3, 87-92 cm). In thin sections, serpentinite clasts are aligned and rotated between coalescent veins filled with a serpentine-like mineral, locally identified as iowaite on board. This suggests that such shear zones may initiate in zones of preferential hydrothermal fluid circulation. The dip of the shear zones (30°) is generally lower than that of the brittle fractures. The obliquity between shear bands and schistosity, when well expressed, indicates a normal shear sense.

Locally in the brecciated intervals where the proportion of serpentine matrix is high, the rounded clasts have been rotated in the soft matrix. Such intense shear zones acted during extensional deformation as ball bearings along 45° dipping planes (Fig. 10; Sample 149-

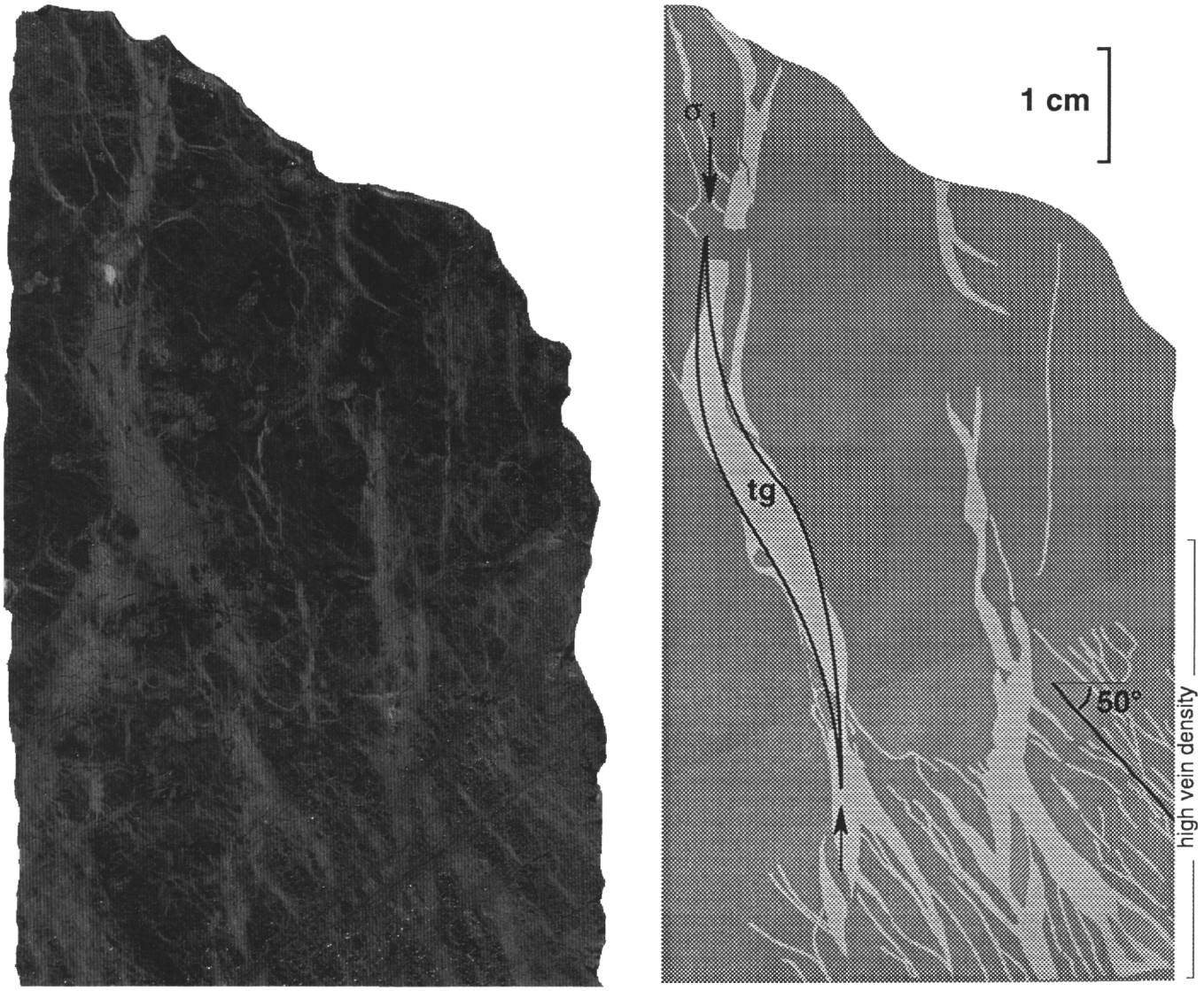

Figure 6. Sigmoidal tension gashes (tg) filled with fibrous pale green serpentine, which have a geometry in accordance with horizontal extension (σ_1 = maximum main strength axis), grading into an anastomosing vein pattern in the lower part of the figure; Sample 149-897C-70R-2, 53-61 cm.

897D-17R-4, 42-60 cm). Friable serpentinite breccias are also sheared in Sections 149-897C-66R-1 to 3 and 897D-18R-2 to 4. Rare clasts of calcite are embedded in these soft sheared breccias (Sample 149-897C-66R-1, 84-90 cm). Calcite crystals display mechanical twins in rare, narrow shear zones in the calcitized upper part of Hole 897D (e.g., Samples 149-897D-10R-3, 15-19 cm, and 14R-3, 43-46 cm). This shows that although calcite-filled fracturing seems generally to be the latest major tectonic event, some shear deformation occurred locally during or after calcite crystallization.

DISCUSSION

Tectono-metamorphic Evolution

According to this study and the joint petrological characterization (Cornen et al., chapter 21, this volume), the serpentinized peridotites underwent three major high-temperature events and a complex structural evolution under subsurface conditions during their uplift:

1. Ductile shear deformation occurred between 1000° and 900°C. It induced a porphyroclastic texture in the rocks, mainly characterized by low recrystallization, the occurrence of kink bands in olivine and orthopyroxene porphyroclasts, and bending of exsolution lamellae in clinopyroxene porphyroclasts. Such features were observed both in the websteritic bandings and the surrounding peridotite. The influence of the initial lithologic heterogeneity on the deformation is difficult to evaluate, because of the pervasive serpentinization of the peridotites and the later evolution of the rocks, which has partly overprinted the primary features. Studies of ophiolite massifs show, however, that websteritic bands, which are more resistant than the surrounding peridotite, tend to form boudins relatively preserved from deformation.
2. Limited partial melting is demonstrated by the residual character of the peridotites, the poikilitic habit of many of the pyroxene crystals, and locally by the presence of a relatively high proportion of plagioclase (up to 35%). Plagioclase occurs as interstitial patches or veinlets that locally pervasively invade the rocks. However, the veinlets generally mark a fabric in the rocks (foliation and lineation) that is concordant with the high-temperature foliation and lineation. These textural relationships suggest that plagioclase melt crystallization occurred at

the end of, and after, the high-temperature shear deformation.

A subsolidus reequilibration of the websterite occurred in plagioclase facies conditions (i.e., at pressures below 1 GPa). This is shown by the crystallization of secondary olivine and orthopyroxene crystals, which are closely associated with plagioclase between, or in the exsolution lamellae of. former pyroxenes. Compositional variations observed in spinels and clinopyroxenes also support this textural evidence (Cornen et al., chapter 21, this volume). In the websterites, although kink-band formation preceded resorption of the pyroxenes, some secondary orthopyroxene crystals are kinked and the associated plagioclase displays mechanical twins. This suggests that reequilibration in the plagioclase field occurred at the end of, and after, the high-temperature deformation event, as plagioclase melt crystallization.

3. Mylonitic and ultramylonitic shear deformation is poorly developed and highly heterogeneous, and it clearly overprints the porphyroclastic texture. It occurred at a relatively low temperature (about 700°C, using the pyroxenes geothermometer [Cornen et al., chapter 21, this volume] and by reference to the temperature estimated for Leg 103 mylonites [Girardeau et al., 1988]) by plastic flow in a shear regime under high-stress conditions in the plagioclase stability field (i.e., under lithospheric physical conditions). This deformation is restricted to a few shear zones developed in plagioclase-rich facies, including the development of a mylonitic foliation that is locally crosscut by ultramylonitic bands. The mylonitic deformation is coaxial with the previous higher temperature deformation event.
4. Ubiquitous low-temperature deformation occurred under subsurface conditions during the serpentinization of the rocks. This heterogeneous deformation, aided by hydrothermal fluid circulation, occurred as a continuum during horizontal extension in a rotational regime. It is expressed either as fracturing or ductile shearing in serpentine-rich zones, and it brecciated the rocks over thick intervals. The dominant fracture-filling mineral progressively changes downward from calcite to serpentine. The deformation was initiated as serpentine-filled fracturing and brecciation. It graded locally into shear zone development where vein density is high. Some intense, generally low-dipping shear zones (about 30°) may have accommodated large displacements in the basement. Although locally sheared, calcite veins are generally the latest major features.

Implications for the Formation of the Margin and Comparison with Galicia Margin

The high-temperature structural evolution of the serpentinized peridotite during the uplift of the mantle shows that, concerning physical conditions and probably also kinematics, the rocks underwent a continuum of deformation at decreasing temperature, under coeval increasing deviatoric stress and decreasing pressure. However, plagioclase melt crystallization occurred at the end of the high-temperature ductile deformation and ended at least partly under static conditions, as attested to by the interstitial habit of the plagioclase veinlets. This suggests that (1) during magma circulation, the mantle sampled at Site 897 was preserved from deformation, possibly as a boudin, and (2) at that time, the shear deformation was localized elsewhere in weaker decoupling layers. The gabbros drilled at Site 900, which were highly sheared at high-temperature under granulite facies conditions (Cornen et al., chapter 26, this volume), may be such a decoupling layer, which existed either as melt products underplated at the base of the crust or as a layer trapped in the uppermost mantle. Because the subsequent mylonitic deformation was poorly developed in the peridotite, the transfer of deformation possibly was effective until the end of ductile deformation in the mantle. The structural evolution of the basement rocks recovered at the ocean/continent transition in the Iberia Abyssal Plain confirms, anyway, that shear deformation is

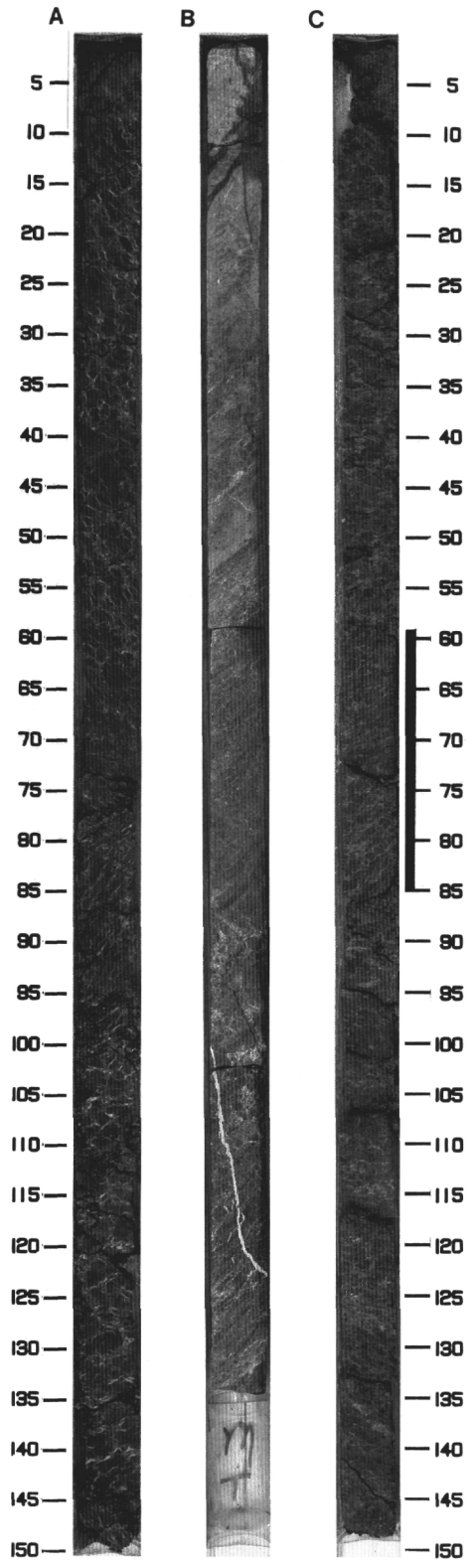

Figure 7. **A.** Thin contorted veins filled with serpentine that permeate and brecciate the serpentinized peridotite. Note the variation of the veins' attitude from dipping at 60° between 0 and 95 cm to subhorizontal or poorly oriented between 100 and 150 cm (Section 149-897C-73R-3). **B.** The same brecciated texture as in (A) is well-preserved between 80 and 135 cm, although later calcite/brucite fracturing extensively overprints previous features (Section 149-897D-17R-4). **C.** The same brecciated texture as in (A) in friable serpentinite breccias (Section 149-897D-10R-2).

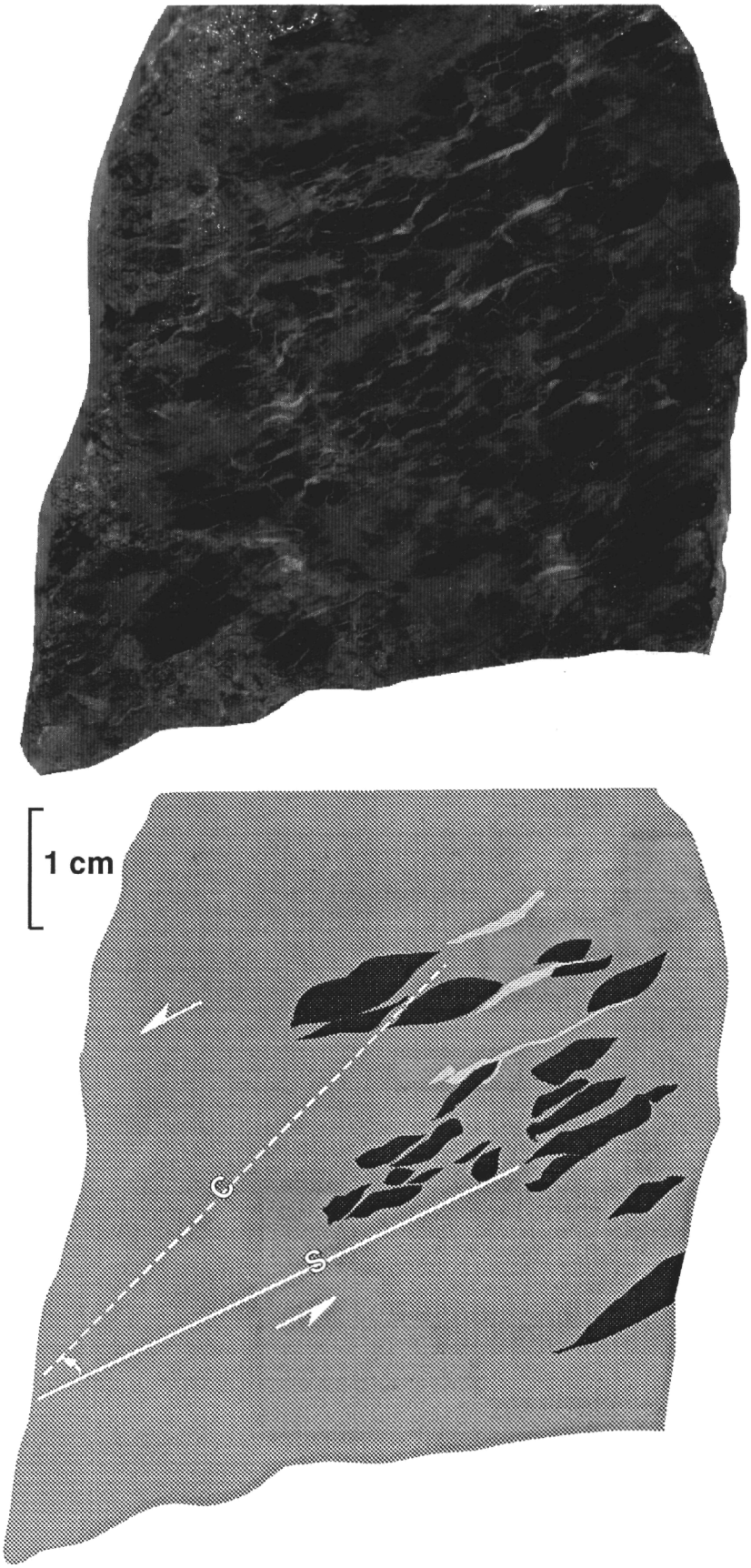

Figure 8. S/C fabric in a shear zone in serpentine-rich Sample 149-897C-71R-2, 115-121 cm. The obliquity between shear bands (C) and schistosity (S) suggests a normal shear sense.

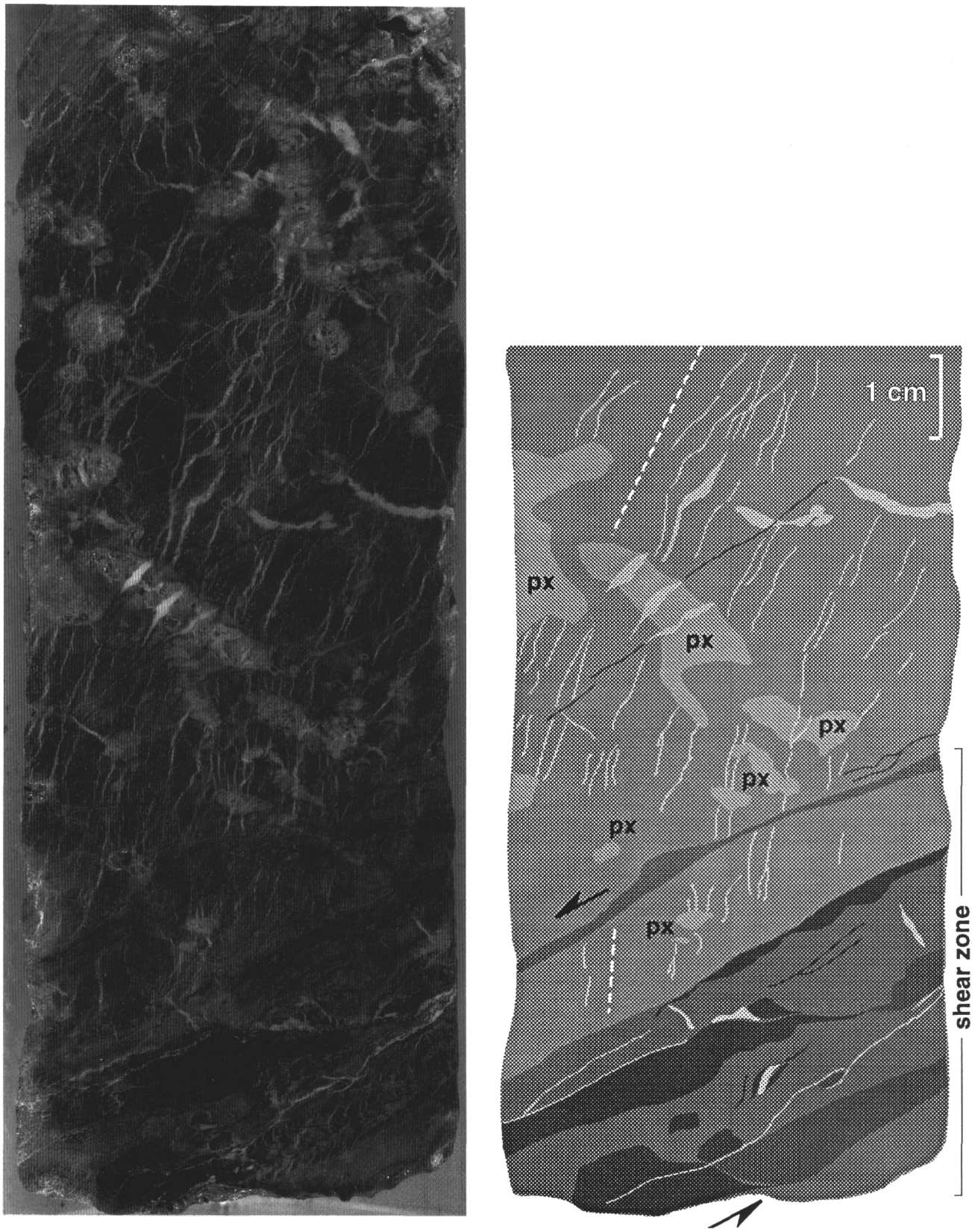

Figure 9. Low-dipping shear zone in bluish serpentinite (108-114 cm); the change of the mean dip of the white serpentine veins (dashed line) from 65° at the top of the sample to subvertical near the shear zone, as well as some poorly developed shear criteria in the shear zone, suggests a normal shear sense (Sample 149-897D-21R-2, 99-114 cm).

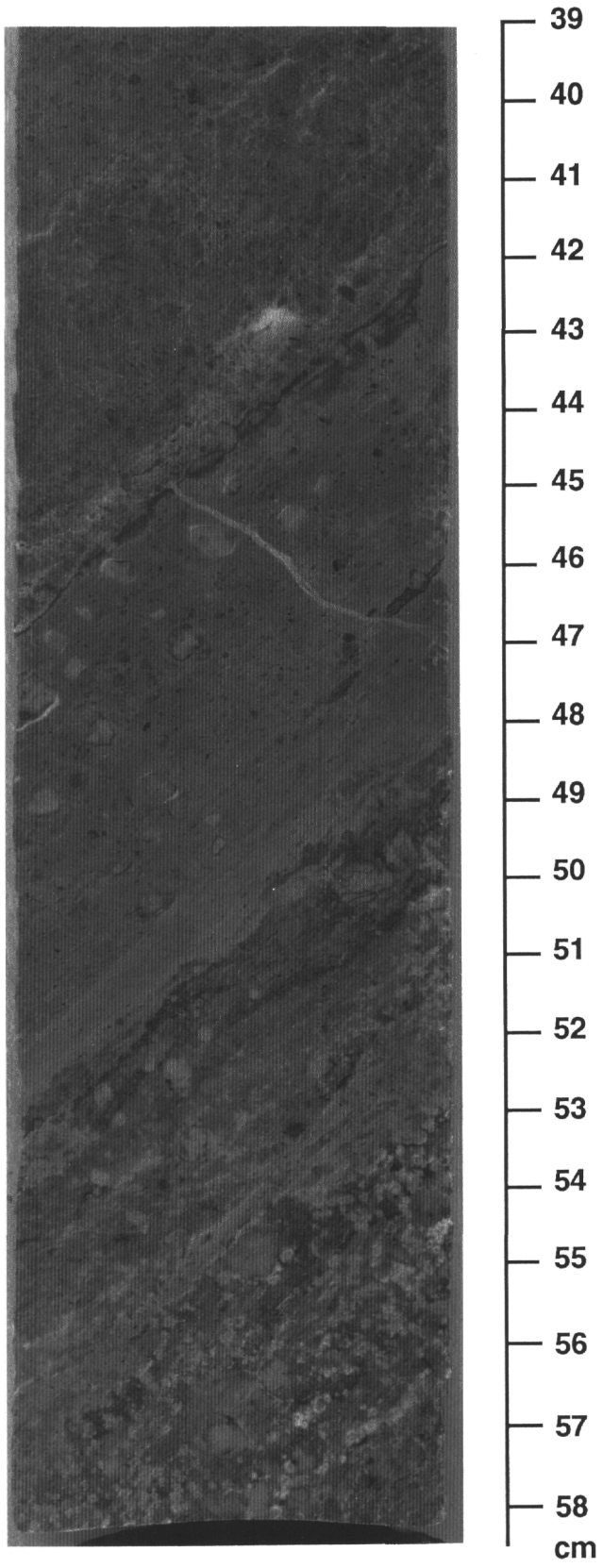

Figure 10. Intense shear zone, dipping at 40°, in a serpentine-rich zone embedded in a calcitized breccia; Sample 149-897D-17R-4, 40-58 cm.

a major mechanism of stretching and thinning of the lithosphere during a rifting episode.

On the Galicia Margin, the peridotite underwent an intense mylonitic deformation (Girardeau et al., 1988; Beslier et al., 1990), which is here, as previously noted, more discrete. This is the main difference in the high-temperature evolution of the Galicia Margin and that of the Site 897 peridotites, which in other respects occurred under similar conditions on both segments of the margin.

Although reorientation of the Site 897 cores in the geographical frame is not possible, the foliation dip and lineation pitch show that the attitude of the high-temperature structures is highly variable (Fig. 3). The most rational explanation is that they have been highly disturbed by further ubiquitous late deformation observed at every depth in the recovered cores. The rotational regime of deformation along late shear zones may have rotated the primary features. This can explain, in particular, the possible observed shear sense reversal.

The late low-temperature deformation highlights the importance of hydrothermalism during the late evolution of the mantle. Hydrothermalism is indeed responsible for the progressive serpentinization of the mantle and also aids fracturing of the rocks. This induces a strong heterogeneity into the mantle by increasing the proportion of serpentine in the rocks, especially along channels of fluid circulation. At Site 897, in the less serpentinized areas, the rocks kept the same brittle behavior during the entire late extension, as in the upper calcitized basement, where calcitization tends to harden the rocks. With an increasing proportion of serpentine, which is a highly ductile material even at low temperatures, the rheological behavior of the rocks progressively changed from brittle to ductile during further extension. This change in deformation mode, as well as the superposed fractures sets, is evidence for a complex and long structural evolution of the basement under subsurface conditions (i.e., at the end of continental rifting) that probably began before emplacement of the mantle on the seafloor, as deep fluid circulation can occur in rifted zones (down to 8-10 km). Calcite-filled fracturing probably occurred mainly after continental breakup, when the first sediments were deposited on mantle rocks exposed on the seafloor.

The late low-temperature deformation documents the late emplacement stages of the mantle on the seafloor at the paleo-rift axis at the end of the continental rifting. One main result of ODP Leg 149 is the demonstration that the ocean/continent transition of nonvolcanic passive margins can be a zone as wide as 150 km, where ultramafic and mafic rocks lie directly under the sedimentary cover (Fig. 11; Shipboard Scientific Party, 1993; Sawyer, Whitmarsh, Klaus, et al., 1994; Beslier et al., 1994). On the Lusigal 12 multichannel seismic line, which provides a cross section of the margin, basement in the ocean/continent transition forms structural highs and basins (Beslier et al., 1993; 1995; Beslier, this volume). Actually, the structural highs do not display the typical asymmetric geometry of tilted continental blocks. On a map, these structures are not as well organized as on the adjacent Galicia Margin, but seem to be grossly parallel and north-south trending (Beslier et al., 1993). As the first continental crust occurrence is suspected to lie to the east at Site 901 (Fig. 11), this high-and-basin structure developed after continental breakup was complete. Sedimentary intervals of Unit IV, tentatively interpreted as mass-flow deposits at the top of the basement, yield ages that become younger upward and range from late Hauterivian to early Aptian (Sawyer, Whitmarsh, Klaus, et al., 1994). Accordingly, the tectonism of the exposed mantle may have lasted at least 10 Ma after the completion of continental breakup. Moreover, deformation may have continued after the Aptian, which would explain the position of such a gravitationally deposited unit at the top of the Site 897 high.

The complex low-temperature structural history of the mantle is in agreement with this long-lasting late tectonism of the basement in the ocean/continent transition. It can account for a polyphase complex tectonism, compatible with the chaotic geometry of the highs in the ocean/continent transition. This suggests that, after tectonic den-

udation at a rift axis, the mantle can be extended over a large width after continental breakup.

The ocean/continent transition to the north on the adjacent Galicia Margin is narrower, as the first continental tilted block is located only 30 km east of the peridotite ridge (Fig. 11; Boillot, Winterer, Meyer, et al., 1988; Boillot et al., 1988a). The late evolution of the peridotite seems to be less complex here than at Site 897, with only serpentine- and calcite-filled fracturing (Girardeau et al., 1988). This suggests that stretching of the exposed mantle was not so ubiquitous along the Galicia Margin as in the Iberia Abyssal Plain. Moreover, the continental breakup occurred during the late Aptian on the Galicia Margin. This shows that the denuded mantle was stretched in the Iberia Abyssal Plain during the last stages of crustal thinning in the Galicia rift.

CONCLUSIONS

Drilling of mantle rocks in the Iberia Abyssal Plain at Site 897 confirmed that the peridotite ridge, first explored on the Galicia Margin, is a major feature that borders the margin over more that 250 km in the ocean/continent transition. As on the Galicia Margin, the evolution of the serpentinized peridotites in the Iberia Abyssal Plain is compatible with adiabatic uplift of a mantle dome during lithospheric stretching, and simple shear is a major mechanism of stretching and thinning of the lithosphere during continental rifting. However, the peridotite in the Iberia Abyssal Plain underwent a more complex evolution under subsurface conditions during the last emplacement of the tectonically denuded mantle dome on the seafloor. This study points out the important role of hydrothermal activity during this late deformation. This late evolution suggests that, after tectonic denudation at a rift axis, the mantle can be stretched over a large width after continental breakup, thus creating a wide ocean/continent transition along the passive margin.

ACKNOWLEDGMENTS

We would like to thank the crews and ODP marine technicians for their skillfulness on board and Roland Derval and Yves Descatoire for their efficiency and technical help, and Fran9oise Boudier and John Ross for helpful reviews of the manuscript. This work was supported by INSU-ODP France-Océanoscope. This is Contribution no. 680 of the "Groupe d'Etude de la Marge Continentale et de 1'Océan" (GEMCO), URA 718-CNRS and University of Paris VI.

REFERENCES

Agrinier, P., Mével, C., and Girardeau, J., 1988. Hydrothermal alteration of the peridotites cored at the ocean/continent boundary of the Iberian Margin: petrologic and stable isotope evidence. *In* Boillot, G., Winterer, E.L., et al., *Proc. ODP, Sci. Results,* 103: College Station, TX (Ocean Drilling Program), 225-234.

Beslier, M.O., 1991. Formation des marges passives et remontée du manteau: modélisation expérimentale et exemple de la marge de la Galice. *Mem. Doc. Cent. Arm. Et. Struct. Socles, Rennes,* 45.

Beslier, M.-O., Ask, M., and Boillot, G., 1993. Ocean-continent boundary in the Iberia Abyssal Plain from multichannel seismic data. *Tectonophysics,* 218:383-393.

Beslier, M.O., and Brun, J.P., 1991. Boudinage de la lithosphère et formation des marges passives. *C.R. Acad. Sci. Ser. 2,* 313:951-958.

Beslier, M.O., Cornen, G., Sawyer, D.S., Whitmarsh, R.B., Klaus, A., Collins, E.S., Comas, M.C., de Kaenel, E., Gervais, E., Gibson, I., Harry, D.L., Hobart, M., Kanamatsu, T., Krawczyk, C.M., Liu, L., Lofts, J.C., Marsaglia, K.M., Meyers, P.A., Milkert, D., Milliken, K.L., Morgan, J.K., Pinheiro, L., Ramirez, P., Seifert, K.E., Shaw, T., Wilson, C., Yin, C., and Zhao, X., 1994. Péridotites et gabbros à la transition continent-océan d'une marge passive: résultats préliminaires du leg ODP 149 dans la Plaine Abyssale Ibérique. *C.R. Acad. Sci. Ser. 2,* 319:1223-1229.

Beslier, M.-O., Girardeau, J., and Boillot, G., 1990. Kinematics of peridotite emplacement during North Atlantic continental rifting, Galicia, NW Spain. *Tectonophysics,* 184:321-343.

Beslier, M.-O., Bitri, A., and Boillot, G., 1995. Structure de la transition continent-océan d'une marge passive: sismique refléxion multitrace dans la Plaine Abyssale Ibérique (Portugal). *C.R. Acad. Sci. Ser. 2,* 320:969-976.

Boillot, G., Comas, M.C., Girardeau, J., Kornprobst, J., Loreau, J.P., Malod, J., Mougenot, D., and Moullade, M., 1988a. Preliminary results of the Galinaute cruise: dives of the submersible Nautile on the western Galicia margin, Spain. *In* Boillot, G., Winterer, E.L., et al., *Proc. ODP, Sci. Results,* 103: College Station, TX (Ocean Drilling Program), 37-51.

Boillot, G., Féraud, G., Recq, M., and Girardeau, J., 1989. "Undercrusting" by serpentinite beneath rifted margins: the example of the west Galicia margin (Spain). *Nature,* 341:523-525.

Boillot, G., Girardeau, J., and Kornprobst, J., 1988b. Rifting of the Galicia Margin: crustal thinning and emplacement of mantle rocks on the seafloor. *In* Boillot, G., Winterer, E.L., et al., *Proc. ODP, Sci. Results,* 103: College Station, TX (Ocean Drilling Program), 741-756.

Boillot, G., Grimaud, S., Mauffret, A., Mougenot, D., Kornprobst, J., Mergoil-Daniel, J., and Torrent, G., 1980. Ocean-continent boundary off the Iberian margin: a serpentinite diapir west of the Galicia Bank. *Earth Planet. Sci. Lett.,* 48:23-34.

Boillot, G., Winterer, E.L., et al., 1988. *Proc. ODP, Sci. Results,* 103: College Station, TX (Ocean Drilling Program).

Bonatti, E., Hamlyn, P., and Ottonello, G., 1981. Upper mantle beneath a young oceanic rift: peridotites from the island of Zabargad (Red Sea). *Geology,* 9:474-479.

Bonatti, E., Ottonello, G., and Hamlyn, P.R., 1986. Peridotites from the island of Zabargad (St. John), Red Sea: petrology and geochemistry. *J. Geophys. Res.,* 91:599-631.

Bonatti, E., Seyler, M., Channell, J., Girardeau, J., and Mascle, G., 1990. Peridotites drilled from the Tyrrhenian Sea, ODP Leg 107. *In* Kastens, K.A., Mascle, J., et al., *Proc. ODP, Sci. Results,* 107: College Station, TX (Ocean Drilling Program), 37-47.

Carter, N.L., 1976. Steady state flow of rocks. *Rev. Geophys. Space Phys.,* 14:301-360.

Carter, N.L., and Avé Lallemant, H.G., 1970. High-temperature flow of dunite and peridotite. *Geol. Soc. Am. Bull.,* 81:2181-2202.

Chian, D., Louden, K.E., Keen, C.E., and Reid, I., 1994. The structure of the conjugate margins of the Labrador Sea based on coincident MCS and wide-angle seismic profiles. *Ann. Geophys.,* Part I, Suppl. I to vol. 12, C36.

Evans, C.A., and Girardeau, J., 1988. Galicia Margin peridotites: undepleted abyssal peridotites from the North Atlantic. *In* Boillot, G., Winterer, E.L., et al., *Proc. ODP, Sci. Results,* 103: College Station, TX (Ocean Drilling Program), 195-207.

Féraud, G., Girardeau, J., Beslier, M.O., and Boillot, G., 1988. Datation $^{39}Ar/^{40}Ar$ de la mise en place des péridotites bordant la marge de la Galice (Espagne). *C. R. Acad. Sci. Ser. 2,* 307:49-55.

Fryer, P., Pearce, J.A., Stokking, L.B., et al., 1990. *Proc. ODP, Init. Repts.,* 125: College Station, TX (Ocean Drilling Program).

Girardeau, J., Evans, C.A., and Beslier, M.-O., 1988. Structural analysis of plagioclase-bearing peridotites emplaced at the end of continental rifting: Hole 637A, ODP leg 103 on the Galicia Margin. *In* Boillot, G., Winterer, E.L., et al., *Proc. ODP, Sci. Results,* 103: College Station, TX (Ocean Drilling Program), 209-223.

Kastens, K., Mascle, J., Auroux, C., Bonatti, E., Broglia, C., Channel, J., Curzi, P., Emeis, K.C., Glaçon, G., Hasegawa, S., Hieke, W., Mascle, G., McKoy, F., McKenzie, J., Mendelson, J., Muller, C., Rehault, J.P., Robertson, A., Sartori, R., Sprovieri, R., and Torii, M., 1986. La campagne 107 du Joides Resolution (Ocean Drilling Program) en Mer Tyrrhénienne: premiers résultats. *C. R. Acad. Sci. Ser. 2,* 303:391-396.

Kent, D.V., and Gradstein, F.M., 1986. A Jurassic to Recent chronology. *In* Tucholke, B.E., and Vogt, P.R. (Eds.), *The Geology of North America: The Western Atlantic Region.* Geol. Soc. Am. DNAG Ser., 1:45-50.

Lallemand, S., Mazé, J.P., Monti, S., and Sibuet, J.C., 1985. Présentation d'une carte bathymétrique de l'Atlantique Nord-Est. *C. R. Acad. Sci. Ser. 2,* 300:145-149.

Lemoine, M., Tricart, P., and Boillot, G., 1987. Ultramafic and gabbroic ocean floor of the Ligurian Tethys (Alps, Corsica, Apennines): in search of a genetic model. *Geology,* 15:622-625.

Mauffret, A., and Montadert, L., 1987. Rift tectonics on the passive continental margin of Galicia (Spain). *Mar. Pet. Geol.,* 40:49-70.

Mercier, J.-C.C, 1985. Olivines and pyroxenes. *In* Wenk, H.R. (Ed.), *Preferred Orientation in Deformed Metals and Rocks: An Introduction to Modern Texture Analyses:* New York (Academic Press), 407-430.

Mougenot, D., 1989. Geologia da margem portuguesa. *Doc. Tecn., Inst. Hidrogr.,* Lisboa, Portugal.

Nicholls, LA., Ferguson, J., Jones, H., Marks, G.P., and Mutter, J.C., 1981. Ultramafic blocks from the ocean floor southwest of Australia. *Earth Planet. Sci. Lett.,* 56: 362-374.

Nicolas, A., Achauer, U., and Daignières, M., 1994. Rift initiation by lithospheric rupture. *Earth Planet. Sci. Lett.,* 123:281-298.

Nicolas, A., Boudier, F., Lyberis, N., Montigny, R., and Guennoc, P., 1985. L'île de Zabargad (Saint -Jean): témoin-clé de l'expansion précoce en Mer Rouge. *C. R. Acad. Sci. Ser. 2,* 301:1063-1068.

Nicolas, A., Boudier, F., and Montigny, R., 1987. Structure of Zabargad island and early rifting of the Red Sea. *J. Geophys. Res.,* 92:461-474.

Nicolas, A., and Poirier, J.-P., 1976. *Crystalline Plasticity and Solid State Flow in Metamorphic Rocks:* New York (Wiley).

Peters, T., and Stettler, A., 1987. Radiometric age, thermobarometry and mode of emplacement of the Totalp peridotite in the Eastern Swiss Alps. *Schweiz. Mineral. Petrogr. Mittel.,* 67:285-294.

Pinheiro, L.M., Whitmarsh, R.B., and Miles, P.R., 1992. The ocean-continent boundary off the western continental margin of Iberia, II. Crustal structure in the Tagus Abyssal Plain. *Geophys. J. Int.,* 109:106-124.

Sawyer, D.S., Whitmarsh, R.B., Klaus, A., et al., 1994. *Proc. ODP, Init. Repts.,* 149: College Station, TX (Ocean Drilling Program).

Shipboard Scientific Party [ODP Leg 149], 1993. ODP drills the West Iberia rifted margin. *Eos,* 74:454-455.

Sibuet, J.-C, Mazé, J.-P., Amortila, P., and Le Pichon, X., 1987. Physiography and structure of the Western Iberian Continental Margin off Galicia, from Sea Beam and seismic data. *In* Boillot, G., Winterer, E.L., Meyer, A.W., et al., *Proc. ODP, Init. Repts.,* 103: College Station, TX (Ocean Drilling Program), 77-98.

Styles, P., and Gerdes, K., 1983. St John's Island (Red Sea): a new geophysical model and its implications for the emplacement of ultramafic rocks in fracture zones and at continental margins. *Earth Planet. Sci. Lett.,* 65:353-368.

Whitmarsh, R.B., Miles, P.R., and Mauffret, A., 1990. The ocean-continent boundary off the western continental margin of Iberia, I. Crustal structure at40°30'N. *Geophys. J. Int.,* 103:509-531.

Whitmarsh, R.B., Pinheiro, L.M., Miles, P.R., Recq, M., and Sibuet, J.C., 1993. Thin crust at the western Iberia ocean-continent transition and ophiolites. *Tectonics,* 12:1230-1239.

Date of initial receipt: 17 January 1995
Date of acceptance: 17 July 1995
Ms 149SR-218

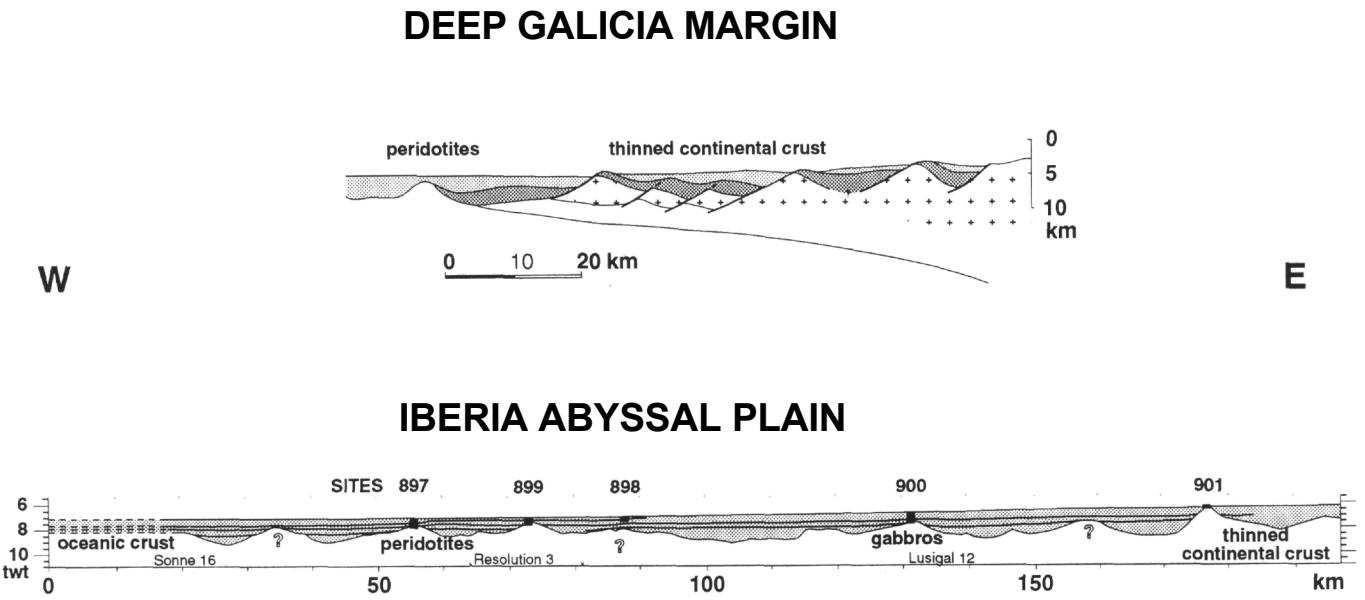

Figure 11. Synthetic cross sections through the deep Galicia Margin (after Boillot et al., 1988b) and the ocean/continent transition of the Iberia Abyssal Plain.

1

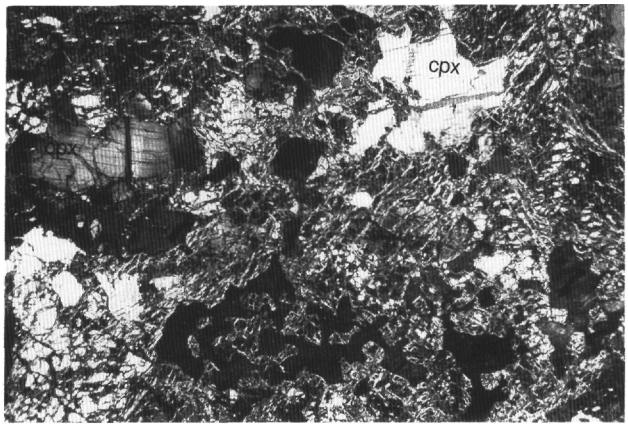

2

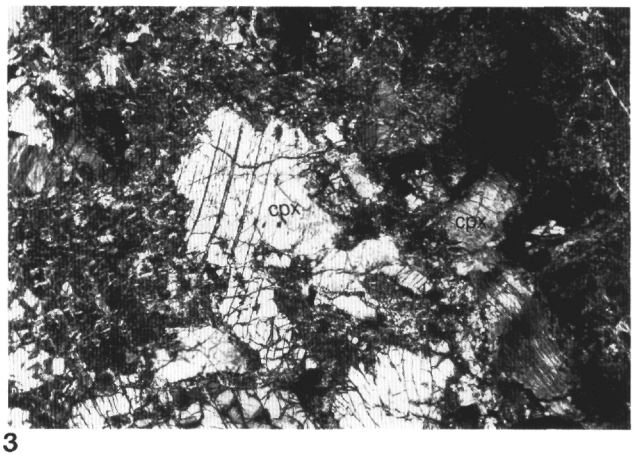

3

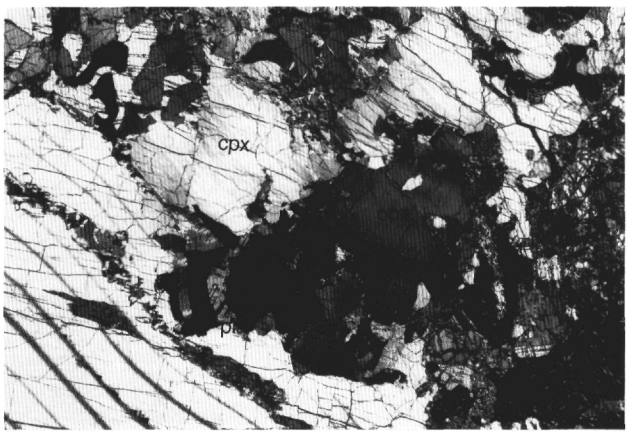

4

5

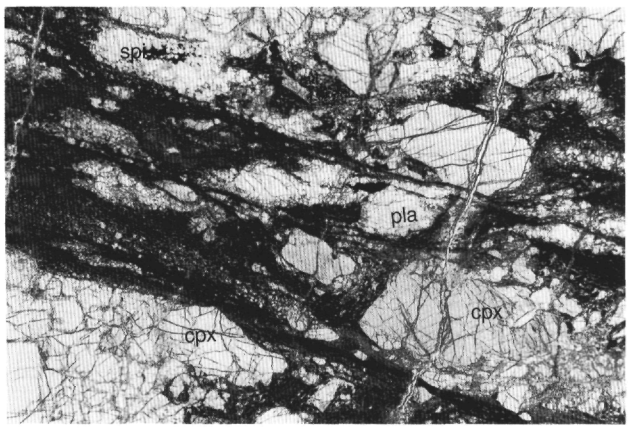

6

Plate 1. Photomicrographs between crossed polars, except Fig. 6 in plane polarized light; opx = orthopyroxene, cpx = clinopyroxene, spi = spinel, pla = plagioclase; S_0 = high-temperature porphyroclastic foliation, S_1 = mylonitic foliation, C = ultramylonitic shear bands. **1.** Porphyroclastic websterite; kinked orthopyroxene lately resorbed and large orthopyroxene porphyroclast slightly elongated by gliding along the (100) plane marked by exsolution lamellae; and spinel-plagioclase foliation concordant with S_0 (Sample 149-897C-67R-2, 141 cm; ×11); **2.** Kinked orthopyroxene and resorbed clinopyroxene in a websterite, with interstitial plagioclase veinlets preferentially aligned parallel to S_0 (Sample 149-67R-2, 27 cm; ×3). **3.** Two clinopyroxene porphyroclasts in a websterite: one is resorbed showing deeply lobate boundaries and the other is highly strained and partially recrystallized at the grain boundary (Sample 149-897C-64R-5, 60 cm; ×13). **4.** Associated plagioclase and pyroxene neoblasts in clinopyroxene exsolution lamellae (Sample 149-897C-64R-5, 100 cm; ×12). **5.** Mylonitic zone in a porphyroclastic websterite; angular relations between S_0, S_1, and C are shown (Sample 149-897C-67R-3, 46 cm; ×9). **6.** Ultramylonitic shear bands in a websterite; S_1 is marked by resorbed spinel in veinlets of recrystallized plagioclase (Sample 149-64R-5, 105 cm; ×11).